The Sound Attenuation Coefficient Optimization in Case of a Three Parameter Impedance Model for a Rectangular 3D Straight Lined Duct of Finite Dimensions

Stefan BALINT[1,2], Agneta M. BALINT*,[1], Robert SZABO[1]

*Corresponding author
[1]Department of Physics, West University of Timisoara
300223 Timisoara, Bulv. V. Parvan 4, Romania
balint@physics.uvt.ro*, robert.szabo@e-uvt.ro
[2]Department of Computer Science, West University of Timisoara
300223 Timisoara, Bulv. V. Parvan 4, Romania
stefanbalint@gmail.com

DOI: 10.13111/2066-8201.2015.7.3.4

Received: 25 July 2015 / Accepted: 13 August 2015

Abstract: *A method for the minimization of the ratio of the sound pressure level at the exit to that at the entrance is presented for a rectangular 3D straight lined duct carrying a uniform gas flow. The duct dimensions, the incident sound wave as well as the frequency of the sound wave propagation are assumed to be known. It is assumed also that the liner impedance model is the mass-spring–damper model. The idea is to compute the considered ratio for a large number of combinations of the values of the inertance, resistance and stiffness of the liner and, by fitting the obtained data, to establish a formula for the dependence of the ratio in discussion on these three parameters of the liner. Using the obtained formula, the minimum value of the ratio, as well as the values of the inertance, resistance and stiffness, for which the minimum is obtained, are found.*

Key Words: *aeroacoustics; acoustic noise attenuation; rectangular 3D lined duct; uniform gas flow; optimization.*

1. INTRODUCTION

Two optimization methods to reduce noise from turbofan aircraft engines by optimizing the acoustic treatment in engine ducts were presented by Astley et al. [1].

In the first method the impedance model is the Helmholz - resonator model and the cost function corresponds to the reduction in radiated far-field sound power over an angular range. “Before the optimization, a large number of computations of the sound pressure level (S.P.L.) is performed. Each run is performed for a specific engine condition and frequency and for a specific value of the liner resistance and reactance. Each computation produces an output data set which contains the S.P.L. at discrete angles on a far-field arc for a single mode which are cut on at the fan plane with unit incident acoustic power. A hard walled solution is also computed for each mode at each frequency and engine condition. This database is used to construct tables of S.P.L. attenuation at discrete polar angles (or integrated over an angular range) in the far field for any defined source combination of

modes at a specific frequency and engine conditions. These S.P.L. attenuation tables are computed for all fan sources and all frequencies in the engine spectrum for a certain grid of resistance and reactance. Since data has only been computed at a discrete grade of resistance and reactance, interpolation is used in the resistance-reactance plane to obtain the S.P.L. – attenuation values in the liner design plane.

So a new set of S.P.L.-attenuation tables was obtained in which the attenuation is tabulated against the liner resistance and reactance at each frequency. The cost function is calculated from this data and contour curves are plotted to indicate optimal values of the liner parameters at a given frequency. In multi-frequency case such calculations are performed after summing contributions over a number of frequency bands using the source power spectrum". According to the authors, beside several advantages "the main disadvantage of the method is that this involves contour plotting to select the minimum value and due to that is limited in practice to a design space defined by two parameters" (two parameter impedance model).

"Where more than two parameters are involved the method can only applied sequentially and there is a doubt that such a process will capture a global optimum."

"In the second optimization method the cost function is evaluated by generating and running C.A.A. models (Anprorad and ACTRAN/TM) in real time. The liner model, which relates liner construction to impedance, is explicitly embedded within the optimization loop and the acoustic solution at each point in the liner design space is obtained by running Anprorad and ACTRAN/TM for given values of resistance and reactance. The Rolls-Royce in-house optimization code SOFT was used. This drives the computation of the CAA solution at a sequence of points in the design space until convergence occurs. In all cases, a global search is performed initially by using a genetic algorithm. This is followed by the application of a gradient based method to locate the optimum".

According to the authors, "the principal advantage of the second method is that in principle it can be applied for an indefinite number of design parameters".

The optimization method presented in our paper is different from those presented in [1]. Our method concerns a three parameter impedance model, namely the mass-spring-damper impedance model. The cost function in our paper is the ratio of the S.P.L. at the exit to that at the entrance.

The S.P.L. attenuation database, computed using the COMSOL Multiphysics software, before the optimization, serves for the construction of a real valued function depending on three variables, which expresses the dependence of the attenuation coefficient on the inertance, resistance and stiffness of the liner.

This function is obtained using the commercial software MathCAD 15, by fitting the data contained in the S.P.L. attenuation database.

The existence of the global minima is assured because for continuous functions defined on a compact set global minima and maxima exist.

These global extremes are captured using MathCAD 15. In preliminaries we precise the concepts, conditions and results which are used in the paper. In the next sections the optimization method is described, a numerical illustration is given followed by some conclusions and comments.

2. PRELIMINARIES

The rectangular 3D straight lined duct of length $L > 0$, thickness h and width l considered in this paper is presented in Fig. 1.

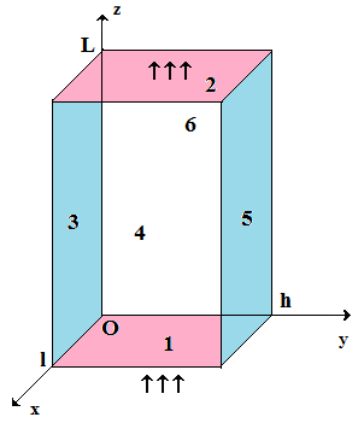

Figure 1: Rectangular 3D straight lined duct

Boundaries 1 and 2 are the entrance and the exit, respectively. Boundaries 3, 4, 5, 6 are the lined walls.

A compressible, inviscid, non-heat conducting, isentropic, perfect gas flows in the duct. It is assumed that the gas flow in the duct is uniform [2]. This means that the functions describing the gas flow are of the form:

$$v_z(x,y,z,t) = U_0 = const. > 0\,,\ v_x(x,y,z,t) = v_y(x,y,z,t) = 0\,,$$

$$p(x,y,z,t) = p_0 = \text{const.} > 0 \text{ and } \rho(x,y,z,t) = \rho_0 = \text{const.} > 0$$

and satisfy - the non-linear Euler equations:

$$\begin{aligned}
&\rho\cdot\left(\frac{\partial v_x}{\partial t} + v_x\cdot\frac{\partial v_x}{\partial x} + v_y\cdot\frac{\partial v_x}{\partial y} + v_z\cdot\frac{\partial v_x}{\partial z}\right) + \frac{\partial p}{\partial x} = 0\\
&\rho\cdot\left(\frac{\partial v_y}{\partial t} + v_x\cdot\frac{\partial v_y}{\partial x} + v_y\cdot\frac{\partial v_y}{\partial y} + v_z\cdot\frac{\partial v_y}{\partial z}\right) + \frac{\partial p}{\partial y} = 0\\
&\rho\cdot\left(\frac{\partial v_z}{\partial t} + v_x\cdot\frac{\partial v_z}{\partial x} + v_y\cdot\frac{\partial v_z}{\partial y} + v_z\cdot\frac{\partial v_z}{\partial z}\right) + \frac{\partial p}{\partial z} = 0\\
&\frac{\partial \rho}{\partial t} + v_x\cdot\frac{\partial \rho}{\partial x} + v_y\cdot\frac{\partial \rho}{\partial y} + v_z\cdot\frac{\partial \rho}{\partial z} + \rho\cdot\left(\frac{\partial v_x}{\partial x} + \frac{\partial v_y}{\partial y} + \frac{\partial v_z}{\partial z}\right) = 0\,,
\end{aligned} \tag{1}$$

- the state equation of the perfect gas

$$p = \rho\cdot R^*\cdot T\,, \tag{2}$$

- the boundary conditions: slip condition on the boundaries 3, 4, 5, 6; and
$v_z(x,y,0,t) = v_z(x,y,L,t) = U_0\,,\ v_x(x,y,0,t) = v_x(x,y,L,t) = 0\,,$
$v_y(x,y,0,t) = v_y(x,y,L,t) = 0$ on the boundaries 1 and 2, respectively,
- the initial condition: $v_z(x,y,z,0) = U_0\,,\ v_x(x,y,z,0) = 0\,,\ v_y(x,y,z,0) = 0\,.$

In equation (1): v_x, v_y, v_z are the velocity field components; p is the pressure field; ρ is the density field. In equation (2): R^* is the gas constant, T is the gas temperature. Equations (1) and (2) are considered for $x \in [0,l]$, $y \in [0,h]$, $z \in [0,L]$ and $t \geq 0$.

The linearized Euler equations (around the considered uniform gas flow) are:

$$\begin{aligned}
&\frac{\partial v'_x}{\partial t} + U_0 \cdot \frac{\partial v'_x}{\partial z} + \frac{1}{\rho_0} \cdot \frac{\partial p'}{\partial x} = 0 \\
&\frac{\partial v'_y}{\partial t} + U_0 \cdot \frac{\partial v'_y}{\partial z} + \frac{1}{\rho_0} \cdot \frac{\partial p'}{\partial y} = 0 \\
&\frac{\partial v'_z}{\partial t} + U_0 \cdot \frac{\partial v'_z}{\partial z} + \frac{1}{\rho_0} \cdot \frac{\partial p'}{\partial z} = 0 \\
&\frac{\partial p'}{\partial t} + c_0^2 \cdot \rho_0 \left(\frac{\partial v'_x}{\partial x} + \frac{\partial v'_y}{\partial y} + \frac{\partial v'_z}{\partial z} \right) + U_0 \cdot \frac{\partial p'}{\partial z} = 0
\end{aligned} \tag{3}$$

where c_0 is the sound speed associated to the uniform flow.

Assume that at a certain moment of time, let say $t = 0$, an acoustic source produces an incident sound wave at the entrance of the duct, (boundary 1) described by the functions $v'_{x_0}(x, y)$, $v'_{y_0}(x, y)$, $v'_{z_0}(x, y)$, $p'_0(x, y)$. The functions: $v'_x = v'_x(x, y, z, t)$, $v'_y = v'_y(x, y, z, t)$, $v'_z = v'_z(x, y, z, t)$, $p' = p'(x, y, z, t)$ describing the incident sound wave propagation in the lined duct verify equations (3) and the initial – boundary condition:

$$\begin{aligned}
&v'_x(x, y, 0, 0) = v'_{x_0}(x, y),\ v'_y(x, y, 0, 0) = v'_{y_0}(x, y),\ v'_z(x, y, 0, 0) = v'_{z_0}(x, y), \\
&p'(x, y, 0, 0) = p'_0(x, y)
\end{aligned} \tag{4}$$

Equations (3) are considered for $x \in [0, l]$, $y \in [0, h], z \in [0, L]$, $t \geq 0$ and the functions v'_{x_0}, v'_{y_0}, v'_{z_0}, p'_0 are assumed continuously differentiable.

If during the propagation the interaction with the liner is of mass-spring-damper type [3], [4], then the normal component $v' = \vec{n} \cdot \vec{v}$ of the velocity on the boundaries 3, 4, 5, 6 verifies the condition:

$$a \cdot \frac{\partial^2 v'}{\partial t^2} + b \cdot \frac{\partial v'}{\partial t} + c \cdot v' = \pm \frac{\partial p'}{\partial t} \tag{5}$$

In (5), the parameters a, b, c are positive real constants and represent: a - inertance, b - resistance, c - stiffness of the liner.

Definition 1. A system of continuously differentiable functions $v'_x = v'_x(x, y, z, t)$, $v'_y = v'_y(x, y, z, t)$, $v'_z = v'_z(x, y, z, t)$, $p' = p'(x, y, z, t)$, defined for $x \in [0, l]$, $y \in [0, h]$, $z \in [0, L]$, $t \geq 0$, which verifies (3) point wise, is called **classical solution** of the system of differential equations (3).

3. THE VELOCITY FIELD POTENTIAL

Proposition 1. If for a classical solution v'_x, v'_y, v'_z, p' of (3) there exists a function Φ_1, differentiable twice such that:

$$v'_x = \frac{\partial \Phi_1}{\partial x},\ v'_y = \frac{\partial \Phi_1}{\partial y} \text{ and } v'_z = \frac{\partial \Phi_1}{\partial z}, \tag{6}$$

then there exists a function Φ differentiable twice, having the property (6) and for which the following equalities hold:

$$\frac{\partial^2\Phi}{\partial t^2}-\left(c_0^2-U_0^2\right)\cdot\frac{\partial^2\Phi}{\partial z^2}-c_0^2\cdot\left(\frac{\partial^2\Phi}{\partial x^2}+\frac{\partial^2\Phi}{\partial y^2}\right)+2\cdot U_0\cdot\frac{\partial^2\Phi}{\partial t\partial z}=0. \tag{7}$$

$$p'=-\rho_0\cdot\left(\frac{\partial\Phi}{\partial t}+U_0\cdot\frac{\partial\Phi}{\partial z}\right). \tag{8}$$

Proof: By using (6) the first, second and third equations of the system of partial differential equations (3) can be written as:

$$\frac{\partial}{\partial x}\left[p'+\rho_0\cdot\left(\frac{\partial\Phi_1}{\partial t}+U_0\cdot\frac{\partial\Phi_1}{\partial z}\right)\right]=0$$

$$\frac{\partial}{\partial y}\left[p'+\rho_0\cdot\left(\frac{\partial\Phi_1}{\partial t}+U_0\cdot\frac{\partial\Phi_1}{\partial z}\right)\right]=0$$

$$\frac{\partial}{\partial z}\left[p'+\rho_0\cdot\left(\frac{\partial\Phi_1}{\partial t}+U_0\cdot\frac{\partial\Phi_1}{\partial z}\right)\right]=0.$$

It follows that there exists a continously differentiable function $\alpha=\alpha(t)$ such that:

$$p'=-\rho_0\cdot\left(\frac{\partial\Phi_1}{\partial t}+U_0\cdot\frac{\partial\Phi_1}{\partial z}\right)+\alpha(t)$$

Defining now the function Φ by

$$\Phi=\Phi_1-\frac{1}{\rho_0}\cdot\int_0^t\alpha(\tau)d\tau$$

Note that Φ verifies (6) and p' verifies (8).

In order, to show that Φ verifies (7), replace p', written in the form (8), in the left hand side of the fourth equation of the system (3) and take into account that Φ verifies (6).

Proposition 2. If a function $\Phi=\Phi(x,y,z,t)$ is continuously differentiable twice for $x\in[0,l]$, $y\in[0,h]$, $z\in[0,L]$, $t\geq 0$ and verifies (7), then the system of functions $v_x'=v_x'(x,y,z,t)$, $v_y'=v_y'(x,y,z,t)$, $v_z'=v_z'(x,y,z,t)$, $p'=p'(x,y,z,t)$, defined by:

$$v_x'=\frac{\partial\Phi}{\partial x},\ v_y'=\frac{\partial\Phi}{\partial y},\ v_z'=\frac{\partial\Phi}{\partial z},\ p'=-\rho_0\cdot\left(\frac{\partial\Phi}{\partial t}+U_0\cdot\frac{\partial\Phi}{\partial z}\right), \tag{9}$$

is a classical solution of the system of partial differential equations (3).

Proof: Replace the functions v_x', v_y', v_z', p' given by (9) into the left hand side of the first, second and third equations of system (3) and find that these equations are satisfied.

Replace now, v_x', v_y', v_z', p', given by (9), in the left hand side of the fourth equation of the system (3), take into account (7) and find that the fourth equation is satisfied.

Definition 2. A function $\Phi=\Phi(x,y,z,t)$ differentiable twice for $x\in[0,l]$, $y\in[0,h]$, $z\in[0,L]$, $t\geq 0$, which verifies point wise the equation (7), is called **velocity field potential** for the system of partial differential equations (3).

***Remarks*: i)** A velocity field potential Φ of system (3) generates a classical solution of (3).

ii) For a classical solution v_x', v_y', v_z', p' of (3) a velocity field potential Φ exists if and only if the following equalities hold:

$$\frac{\partial v_x'}{\partial y} = \frac{\partial v_y'}{\partial x}, \frac{\partial v_x'}{\partial z} = \frac{\partial v_z'}{\partial x}, \frac{\partial v_y'}{\partial z} = \frac{\partial v_z'}{\partial y}.$$

iii) There exist classical solutions of (3) for which velocity field potential doesn't exist. For instance, for the classical solution given by:

$$v_x' = \sin\left[x + y + z - \left(U_0 - c_0\sqrt{3}\right)\cdot t\right] + \cos\left(x + y + z - U_0 \cdot t\right)$$
$$v_y' = \sin\left[x + y + z - \left(U_0 - c_0\sqrt{3}\right)\cdot t\right]$$
$$v_z' = \sin\left[x + y + z - \left(U_0 - c_0\sqrt{3}\right)\cdot t\right] - \cos\left(x + y + z - U_0 \cdot t\right)$$
$$p' = -c_0\rho_0\sqrt{3}\cdot\sin\left[x + +y + z - \left(U_0 - c_0\sqrt{3}\right)\cdot t\right]$$

velocity field potential doesn't exist because

$$\frac{\partial v_x'}{\partial y} - \frac{\partial v_y'}{\partial x} = -\sin\left(x + y + z - U_0 \cdot t\right) \neq 0.$$

In the following sections only classical solutions for which velocity field potential exist will be used.

4. TIME-HARMONIC ANALYSIS AND OPTIMIZATION PROCEDURE

Time-harmonic analysis of the propagation of the incident sound wave consists in the research of the time harmonic velocity field potentials $\Phi(x, y, z, t) = e^{i\omega t}\cdot K(x, y, z)$, which satisfy equation (7), the radiation condition on the boundaries 1, 2 and the impedance condition on boundaries 3, 4, 5, 6. Here ω is the angular frequency $\omega = 2\pi\nu$ and ν is the frequency of the propagating sound wave.

Radiation is a class of non-reflecting boundary conditions which assumes that there is an incoming exciting wave (boundary 1) and optionally an outgoing wave (boundary 2).

The impedance boundary condition describes the interaction of the propagating sound wave with the liner. The input impedance of the liner represents the ratio of pressure to normal velocity, i.e. $Z = \frac{p'}{v'}$. For the lined boundaries 3, 4, 5, 6 the impedance is $Z(\omega) = a\cdot i\cdot\omega + b - \frac{i\cdot c}{\omega}$.

In numerical computation the duct sizes l, h, L, the incident sound velocity field potential, the frequency ν (or $\omega = 2\pi\nu$) of the propagating wave, the gas flow velocity U_0, the density ρ_0, the associated sound speed c_0 as well the liner parameters a, b, c have to be specified. The sound attenuation coefficient optimization procedure, proposed in this paper, is the following:

Step 1. Specify: the sizes L [m], l[m], h[m] of the lined duct; three ranges $[\underline{a}, \bar{a}]$, $[\underline{b}, \bar{b}]$, $[\underline{c}, \bar{c}]$ of interest for the liner parameters a [kg/m^2], b [kg/m^{2}s], c [kg/m^{2}s^2]; the gas flow parameters U_0 [m/s], ρ_0 [kg/m^3]; the associated sound speed c_0 [m/s]; the incident velocity field potential $\Phi(x, y, 0, 0) = K(x, y, 0) = K_0(x, y)$; the frequency ν [Hz] of the propagating sound wave.

Step 2. In the ranges $[\underline{a},\bar{a}]$, $[\underline{b},\bar{b}]$, $[\underline{c},\bar{c}]$ specify l - different values for a; m - different values for b; n - different values for c; respectively, i.e.:

$$\underline{a} < a_1 < a_2 < \ldots < a_l < \bar{a};\ \underline{b} < b_1 < b_2 < \ldots < b_m < \bar{b};\ \underline{c} < c_1 < c_2 < \ldots < c_n < \bar{c}.$$

Step 3. For a combination a_i, b_j, c_k; $i = \overline{1,l}$, $j = \overline{1,m}$, $i = \overline{1,n}$ compute numerically the sound pressure level at the entrance $SP^{(\nu)}_{(a_i b_j c_k)}(x, y, 0)$ and that at the exit $SP^{(\nu)}_{(a_i b_j c_k)}(x, y, L)$ of the duct solving equation (7) using finite element method and determine the sound attenuation coefficient $A^{(\nu)}_{(a_i b_j c_k)}$ at the duct axis defined as:

$$A^{(\nu)}_{(a_i b_j c_k)} = SP^{(\nu)}_{(a_i b_j c_k)}(l/2, h/2, L) / SP^{(\nu)}_{(a_i b_j c_k)}(l/2, h/2, 0).$$

Step 4. Fit the data a_i, b_j, c_k and $A^{(\nu)}_{(a_i b_j c_k)}$ and find the dependence $A^{(\nu)} = A^{(\nu)}(a, b, c)$ of the attenuation coefficient $A^{(\nu)}$ on the liner parameters.

Step 5. Using the obtained dependence $A^{(\nu)} = A^{(\nu)}(a, b, c)$, find the minimum value of the attenuation coefficient $A^{(\nu)}$ as well the values of parameters a, b, c for which the minimum value is obtained.

5. NUMERICAL ILLUSTRATION

Computation was performed using the software COMSOL Multiphysics 3.5.a (for the computation of the attenuation tables data) and MathCAD 15 (for capturing the optimum) in a 3D rectangular geometry for the following numerical data:

$$l = 0.6[m];\ h = 1[m];\ L = 2\,[\text{m}];\ U_0 = 80\,[\text{m/s}];\ \rho_0 = 1.25[\text{kg/m}^3];\ c_0 = 343[\text{m/s}];$$

$$K_0(x, y) = \cos(x) + i \cdot \sin(y)\,[\text{m}^2/\text{s}];\ \nu = 100[\text{Hz}];\ \underline{a} = 0.0715[\text{kg/m}^2];$$

$$\bar{a} = 0.1715[\text{kg/m}^2];\ \underline{b} = 50\,[\text{kg/m}^2\cdot\text{s}];\ \bar{b} = 150\,[\text{kg/m}^2\cdot\text{s}];\ \underline{c} = 7466[\text{kg/m}^2\cdot\text{s}^2];$$

$$\bar{c} = 8766[\text{kg/m}^2\cdot\text{s}^2].$$

By fitting almost 10^4 computed attenuation table data, for the sound attenuation coefficient the following formula was obtained:

$$A^{(100)}(a, b, c) = A_1(b) + A_2(b)\cdot a + A_3(b)\cdot c + A_4(b)\cdot a^2 + A_5(b)\cdot c^2 + A_6(b)\cdot a\cdot c + A_7(b)\cdot a^3 + A_8(b)\cdot c^3 + A_9(b)\cdot a\cdot c^2 + A_{10}(b)\cdot a^2\cdot c$$

with

$$A_1(b) = \frac{0.670610013 - 0.33026362\cdot b^{0.5} + 0.060289694\cdot b - 0.00476563\cdot b^{1.5} + 0.000127866\cdot b^2}{1 - 0.516902368\cdot b^{0.5} + 0.100619694\cdot b - 0.00886948\cdot b^{1.5} + 0.000318401\cdot b^2 - 3.2621\cdot 10^{-6}\cdot b^{2.5}}$$

$$A_2(b) = \frac{-1.07119933 + 0.38505014\cdot b^{0.5} - 0.04696515\cdot b + 0.00213319\cdot b^{1.5} - 1.7444\cdot 10^{-5}\cdot b^2}{1 - 0.6665776\cdot b^{0.5} + 0.179287726\cdot b - 0.02435773\cdot b^{1.5} + 0.001666069\cdot b^2 - 4.6059\cdot 10^{-5}\cdot b^{2.5}}$$

$$A_3(b) = 2.45049\cdot 10^{-5} - \frac{0.01716058}{b} + \frac{5.212477974}{b^2} - \frac{873.597386}{b^3} + \frac{8982219899}{b^4} - \frac{5.7832\cdot 10^6}{b^5} + \frac{2.27517\cdot 10^8}{b^6} - \frac{5.009\cdot 10^9}{b^7} + \frac{4.73276\cdot 10^{10}}{b^8}$$

$$A_4(b) = \frac{-46.6261874 + 17.70776389\cdot b^{0.5} - 2.6840641\cdot b + 0.207596238\cdot b^{1.5} - 0.00819969\cdot b^2 + 0.0001307866\, b^{2.5}}{1 - 0.718237\cdot b^{0.5} + 0.208914777\cdot b - 0.03049745\cdot b^{1.5} + 0.002239836\cdot b^2 - 6.3122\cdot 10^{-5}\cdot b^{2.5}}$$

$$A_5(b) = -5.546\cdot 10^{-9} + \frac{4.17729\cdot 10^{-6}}{b} - \frac{0.00136737}{b^2} + \frac{0.255505560}{b^3} - \frac{30.0455567}{b^4} + \frac{2308.060575}{b^5} - \frac{115934224}{b^6} + \frac{3.675\cdot 10^{6}}{b^7} - \frac{6.6769\cdot 10^{7}}{b^8} + \frac{5.30228\cdot 10^{8}}{b^9}$$

$$A_6(b) = \frac{8.04413\cdot 10^{-6} - 1.1728\cdot 10^{-6}\cdot b^{0.5} + 1.59576\cdot 10^{-8}\cdot b - 5.7069\cdot 10^{-10}\cdot b^{1.5}}{1 - 0.56902357\cdot b^{0.5} + 0.124589394\cdot b - 0.01252585\cdot b^{1.5} + 0.000497673\cdot b^2}$$

$$A_7(b) = \frac{-15.1962764 + 4.046621945\cdot b^{0.5} - 0.3810492\cdot b + 0.013797398\cdot b^{1.5} - 0.00017125\cdot b^2}{1 - 0.70781563\cdot b^{0.5} + 0.203080139\cdot b - 0.02970674\cdot b^{1.5} + 0.002231067\cdot b^2 - 7.0395\cdot 10^{-5}\cdot b^{2.5}}$$

$$A_8(b) = 1.86379\cdot 10^{-14} - 1.33\cdot 10^{-15}\cdot b + 3.9324\cdot 10^{-17}\cdot b^2 - 6.281\cdot 10^{-19}\cdot b^3 + 5.85388\cdot 10^{-21}\cdot b^4 - 3.18\cdot 10^{-23}\cdot b^5 + 9.3082\cdot 10^{-26}\cdot b^6 - 1.1302\cdot 10^{-28}\cdot b^7$$

$$A_9(b) = 2.34826\cdot 10^{-10} - \frac{1.4447\cdot 10^{-7}}{b} + \frac{3.65833\cdot 10^{-5}}{b^2} - \frac{0.00470205}{b^3} + \frac{0.344776011}{b^4} - \frac{14.1574841}{b^5} + \frac{316.901852}{b^6} - \frac{3076.76793}{b^7}$$

$$A_{10}(b) = \frac{-0.00025508 + 7.79388\cdot 10^{-5}\cdot b^{0.5} - 8.8902\cdot 10^{-6}\cdot b + 4.35454\cdot 10^{-7}\cdot b^{1.5} - 7.8845\cdot 10^{-9}\cdot b^2}{1 - 0.58962131\cdot b^{0.5} + 0.133388756\cdot b - 0.01375263\cdot b^{1.5} + 0.000561162\cdot b^2}$$

The minimum of $A^{(100)}(a,b,c)$ is equal to $A^{(100)}_*(a,b,c) = 0.558622145164005$ and is obtained for $a^* = 0.1518478205364879$, $b^* = 50$, $c^* = 8766$. These values of the liner parameters represent the best choose (in the given ranges) and are different from those considered in the literature [5], [6]. For a^*, b^*, c^* the sound pressure level distribution in the 3D rectangular lined duct is represented in Fig. 2.

According to Fig.2, the sound pressure level decreases along the duct length, but the decrease is not uniform. One cause of the no uniformity could be the incident wave. The sound pressure level decrease along the centerline of the duct is presented in Fig. 3. According to Fig. 3, the sound pressure level decreases almost linearly along the duct axis, excepting a small region close to the exit, where the sound pressure level increases.

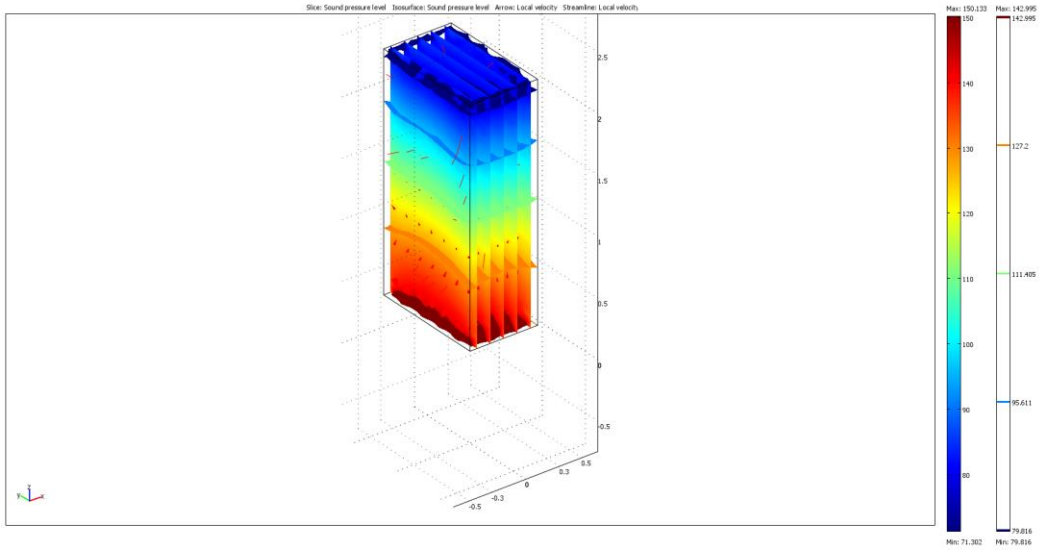

Figure 2: Sound pressure level distribution in the duct.

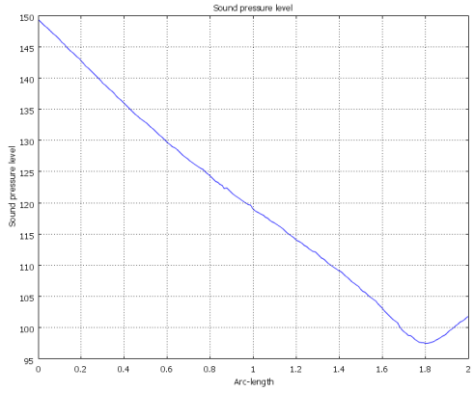

Figure 3: Sound pressure level distribution along the centerline of the duct.

The sound pressure level decrease along the lined walls $x = 0$ [m], $x = 0.6[m]$; $y = 0[m]$; $y = 1[m]$ and along the central line of the walls is presented in Fig. 4. a, b; Fig5. a,b; Fig.6. a,b; Fig.7. a,b; respectively.

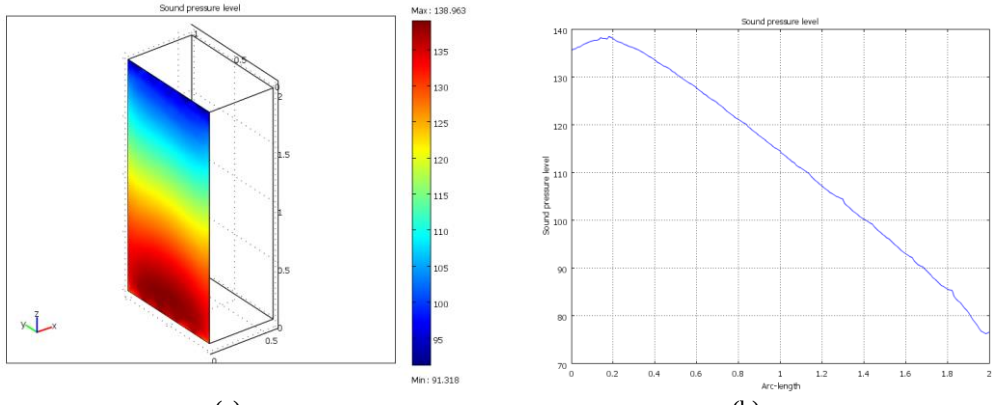

(a) (b)

Figure 4: Sound pressure level decrease along the wall $x = 0$.
(a) distribution along the lined wall; (b) distribution along the center line of the wall.

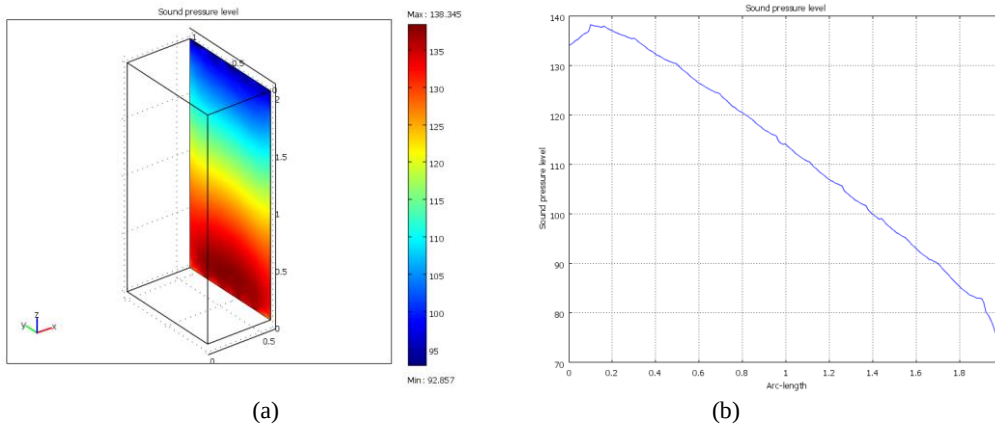

(a) (b)

Figure 5: Sound pressure level decrease along the wall $x = 0.6[m]$.
(a) distribution along the lined wall; (b) distribution along the center line of the wall.

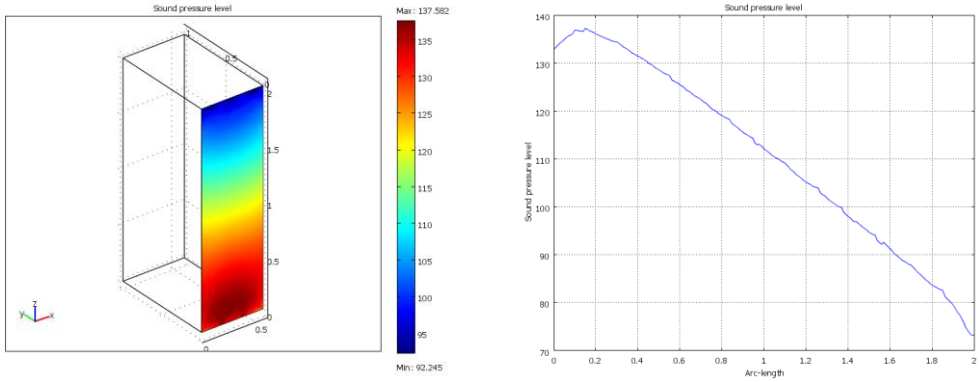

(a) (b)

Figure 6: Sound pressure level decrease along the wall $y = 0[m]$.

(a) distribution along the lined wall; (b) distribution along the center line of the wall.

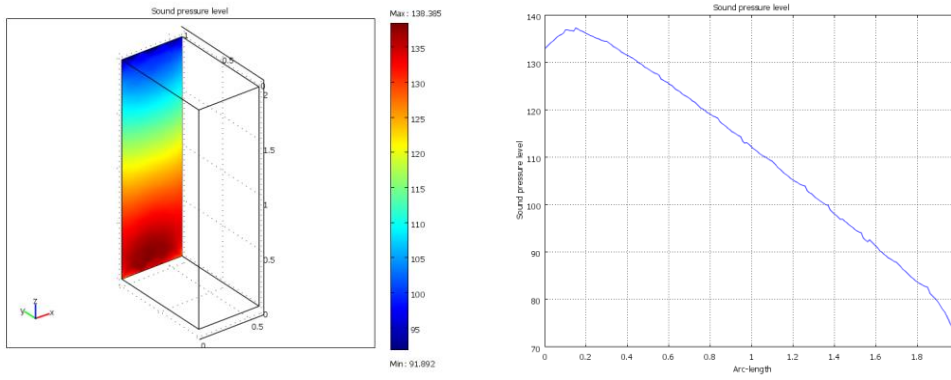

(a) (b)

Figure 7: Sound pressure level decrease along the wall $y = 1[m]$.

(a) distribution along the lined wall; (b) distribution along the center line of the wall.

According to Fig. 4. a, b; Fig. 5. a, b; Fig. 6. a, b; Fig. 7. a, b, the sound pressure level decreases along the lined walls, excepting a small region at the entrance, where it increases.

The sound pressure level distributions at the entrance, at the exit, as well on their diagonal lines, are represented in Figs. 8. a, b and Figs. 9. a, b, respectively.

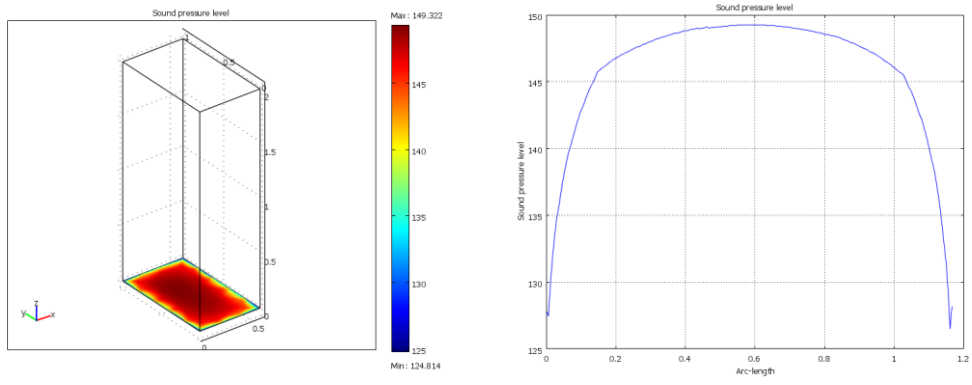

(a) (b)

Figure 8: Sound pressure level at the entrance $z = 0$.

(a) distribution at the entrance; (b) distribution along the diagonal line of the entrance.

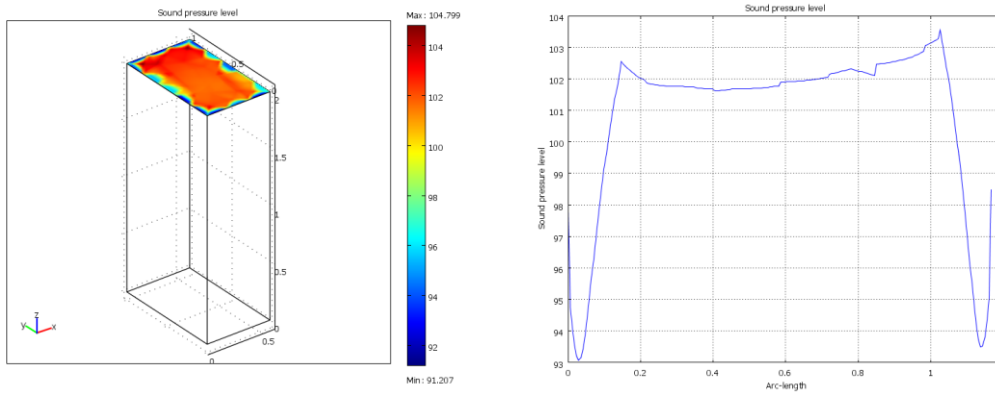

(a) (b)

Figure 9: Sound pressure level at the exit $z = 2[m]$.

(a) distribution at the exit; (b) distribution along the diagonal line of the exit.

According to Figs. 8. a, b, the sound pressure level at the entrance is maximum in the center. According to Fig. 9. a, b, the sound pressure level at the exit has three minimum values: in the center and close to the walls. It can be seen also, that the sound pressure level distribution at the exit is much more complex than at the entrance.

The obtained numerical results are specific; i.e. the obtained values a^*, b^*, c^*, A^* are optimal for the numerical data considered at the beginning. For the obtained a^*, b^*, c^*, the value of the attenuation coefficient A changes if the duct sizes change. Computed results illustrating these changes are given in Table 1.

Table 1: Dependence of the attenuation coefficient on the duct sizes.

l [m]	0.6	0.8	0.4	0.6	0.6	0.6	0.6
h [m]	1	1	1	1.2	0.8	1	1
L [m]	2	2	2	2	2	3	1.5
A	0.5586	0.5175	0.5969	0.5630	0.5688	0.3193	0.6808

6. CONCLUSIONS AND COMMENTS

The optimization procedure, presented in this paper, uses a large number of values of the coefficient of attenuation, computed before the optimization, under the hypothesis that the velocity potential exists. The coefficients of attenuation are computed for a given duct, frequency and incident wave and for a grid of the impedance parameters - resistance, inertance and stiffness - using the acoustic module of the COMSOL Multuphysics software.
The function that represents the dependence of the coefficient attenuation on the three impedance parameters is obtained by using the commercial software MathCAD 15 and fitting the computed coefficients of attenuation. The optimum is found using this function and the same software. The main advantage of this optimization method is that it can be used in case of three parameter impedance models. The disadvantage is that the method is (for the moment) a single frequency method and the mean flow is uniform. The dependence of the optimum on the duct sizes, presented in Table 1, seems to be so strong that motivates a future investigation of the dependence of the optimums a^*, b^*, c^*, A^*, on the duct sizes and an analysis of the significance of results obtained for infinitely long lined ducts.

CONFLICT OF INTERESTS

The authors declare that there is no conflict of interests regarding the publication of this paper.

ACKNOWLEDGMENT

This work was supported by a grant of the Romanian National Authority for Scientific Research, CNCS-UEFISCDI, project number PN-II-ID-PCE-2011-3-0171.

REFERENCES

[1] R. J. Astley, R. Sugimoto and P. Mustafa, Computational aero-acoustics for fan duct propagation and radiation. Current status and application to turbofan liner optimization, *Journal of Sound and Vibration*, vol. **330**, no.16, pp. 3832-3845, 2011.

[2] B. I. Tester, The propagation and the attenuation of sound in lined ducts containing uniform or «plug» flow, *Journal of Sound and Vibration*, vol. **28**, no.2, pp.151-203, 1973.

[3] S. W. Rienstra, Impedance models in time domain including the extended Helmholtz Resonator model, *AIAA paper 2006*-2686 of the 12th AIAA/CEAS Aeroacoustics Conference, Cambridge, MA, USA, 8-10 May 2006.

[4] C. K. W. Tam and L. Auriaoult, Time-domain impedance boundary condition for computational aeroacoustics, *AIAA Journal* vol. **34**, no.5, pp. 917-923, 1996.

[5] S. Balint, A. M. Balint, M. Darau, Linear stability of a non slipping mean flow in a 2-D straight lined duct with respect to modes tipe initial (instantaneous) perturbations, *Applied Mathematical Modelling*, vol. **35** pp.1081-1095, 2011.

[6] S. W. Rienstra and M. Darau, Boundary-layer thickness effects of the hydrodynamic instability along an impedance wall, *Journal of Fluid Mechanics*, vol. **671**, pp.559-573, 2011.